Biometrika (2023), **110**, 2, *pp.* 361–379 https://doi.org/10.1093/biomet/asac055
Advance Access publication 29 September 2022

Additive models for symmetric positive-definite matrices and Lie groups

BY Z. LIN

Department of Statistics and Data Science, National University of Singapore, 21 Lower Kent Ridge Road, 119077 Singapore
linz@nus.edu.sg

H.-G. MÜLLER

Department of Statistics, University of California, Davis, One Shields Avenue, Davis, California 95616, U.S.A.
hgmueller@ucdavis.edu

AND B. U. PARK

Department of Statistics, Seoul National University, 1 Gwanak-ro, Gwanak-gu, Seoul, Republic of Korea
bupark@stats.snu.ac.kr

SUMMARY

We propose and investigate an additive regression model for symmetric positive-definite matrix-valued responses and multiple scalar predictors. The model exploits the Abelian group structure inherited from either of the log-Cholesky and log-Euclidean frameworks for symmetric positive-definite matrices and naturally extends to general Abelian Lie groups. The proposed additive model is shown to connect to an additive model on a tangent space. This connection not only entails an efficient algorithm to estimate the component functions, but also allows one to generalize the proposed additive model to general Riemannian manifolds. Optimal asymptotic convergence rates and normality of the estimated component functions are established, and numerical studies show that the proposed model enjoys good numerical performance, and is not subject to the curse of dimensionality when there are multiple predictors. The practical merits of the proposed model are demonstrated through an analysis of brain diffusion tensor imaging data.

Some key words: Additive regression; Asymptotic normality; Diffusion tensor; Log-Cholesky metric; Log-Euclidean metric; Riemannian manifold; Toroidal data.

1. INTRODUCTION

Data in the form of symmetric positive-definite matrices arise in many areas, including computer vision (Rathi et al., 2007; Caseiro et al., 2012), signal processing (Arnaudon et al., 2013; Hua et al., 2017), medical imaging (Fillard et al., 2007; Dryden et al., 2009) and neuroscience (Friston, 2011), among other fields and applications. For instance, they are used to model brain functional connectivity that is often characterized by covariance matrices of blood-oxygen-level-dependent signals (Huettel et al., 2008). In diffusion tensor imaging analysis (Le Bihan, 1991), a

© The Author(s) 2022. Published by Oxford University Press on behalf of the Biometrika Trust.
All rights reserved. For permissions, please email: journals.permissions@oup.com

Downloaded from https://academic.oup.com/biomet/article/110/2/361/6730723 by University of California, Davis - Library user on 04 July 2023

3×3 symmetric positive matrix that is computed for each voxel describes the dominant shape of local diffusion of water molecules. While the analysis of symmetric positive-definite matrices as responses in a regression model is our primary emphasis in this paper, our results more generally extend to responses with a Lie group structure that include data on the torus.

The space $\mathcal{S}^+$ of symmetric positive-definite matrices is a nonlinear metric space and, depending on the metric, forms a Riemannian manifold. Various metrics have been studied (Pigoli et al., 2014); an important criterion for choosing a metric is to avoid the swelling effect. This refers to the phenomenon that the determinant of the Fréchet mean of a set of symmetric positive-definite matrices may be substantially larger than that of any of the constituent matrices. The swelling effect becomes evident in the geodesics connecting two elements of $\mathcal{S}^+$ (Arsigny et al., 2007), negatively affects specifically the Frobenius metric and various other metrics, and is problematic for many applications. These include diffusion tensor imaging, where a diffusion tensor is represented by a symmetric positive-definite matrix and the determinant quantifies diffusion of the tensor. The swelling effect will then lead to distortions when quantifying diffusion.

The abundance of $\mathcal{S}^+$-valued data in many areas stands in contrast with the relative sparsity of work on their statistical analysis, in particular regarding regression with $\mathcal{S}^+$-valued responses. Existing work includes Riemannian frameworks to analyse diffusion tensor images with a focus on averages and modes of variation (Pennec et al., 2006; Fletcher & Joshib, 2007) and various versions of nonparametric regression such as spline regression (Barmpoutis et al., 2007), local constant regression (Davis et al., 2010), intrinsic local linear regression (Yuan et al., 2012), wavelet regression (Chau & von Sachs, 2019) and Fréchet regression (Petersen et al., 2019). Various metric, manifold and Lie group structures have been proposed, for example, the trace metric (Lang, 1999), affine-invariant metric (Moakher, 2005; Pennec et al., 2006; Fletcher & Joshib, 2007), log-Euclidean metric (Arsigny et al., 2007), log-Cholesky metric (Lin, 2019), scaling-rotation distance (Jung et al., 2015) and Procrustes distance (Dryden et al., 2009). As $\mathcal{S}^+$is a Riemannian manifold and more generally a metric space, regression techniques developed for general Riemannian manifolds (e.g., Pelletier, 2006; Shi et al., 2009; Davis et al., 2010; Steinke et al., 2010; Fletcher, 2013; Hinkle et al., 2014; Cornea et al., 2017, among many others) and metric spaces (Hein, 2009; Chen & Müller, 2022; Lin & Müller, 2021) also apply to $\mathcal{S}^+$.

Additive regression originating with Stone (1985) is known to be an efficient way of avoiding the well-known curse of the dimensionality problem that one faces in nonparametric regression when the dimension of the covariate vector increases, but so far has been by and large limited to the case of real-valued and functional responses. Examples for additive regression approaches for real-valued responses include the original work on smooth back fitting (Mammen et al., 1999) and extensions to generalized additive models (Yu et al., 2008), additive quantile models (Lee et al., 2010), generalized varying coefficient models (Lee et al., 2012), errors in variables (Han & Park, 2018) and functional or distributional responses (Scheipl et al., 2015; Park et al., 2018; Han et al., 2020; Jeon & Park, 2020).

In this paper, we develop an additive regression model for responses residing in a Lie group that includes the space $\mathcal{S}^+$ as the primary example, with an extension to general Riemannian manifolds. This paper contains three major contributions. First, to the best of our knowledge, this is the first paper to study additive regression for $\mathcal{S}^+$-valued responses, counteracting the curse of dimensionality while maintaining a high degree of flexibility. Previous studies for modelling $\mathcal{S}^+$-valued responses focused on unstructured nonparametric regression such as local constant/polynomial regression that are well known to be subject to the curse of dimensionality when there are many predictors.

Second, by focusing on Abelian Lie group-valued responses that include data on the torus (Eltzner et al., 2018), as well as $\mathcal{S}^+$-valued responses, we propose a novel intrinsic group additive

Downloaded from https://academic.oup.com/biomet/article/110/2/361/6730723 by University of California, Davis - Library user on 04 July 2023

regression model that directly exploits the Abelian group structure of the responses. This sets our work apart, as previously only the general manifold structure of responses was considered in the few existing nonadditive regression approaches. To the best of our knowledge, this is the first work to connect additive regression with Lie groups. This connection extends the reach of additive models in a very natural way.

Third, we show that this group additive model can be transformed into an additive model on tangent spaces by utilizing the Riemannian logarithmic map, which paves the way for extending the additive model to the case of responses that lie on more general manifolds. While throughout we showcase the proposed approaches for the space $\mathcal{S}^+$ of symmetric positive-definite matrices with suitable metrics, our results are by no means limited to this type of response, and are applicable to additive regression modelling for a much larger class of manifold-valued responses.

2. Preliminaries on differential geometry

We compile here some basic notions for Riemannian manifolds and Lie groups, referring readers to § S.1 of Shao et al. (2022) for a self-contained note on basic concepts of Riemannian geometry and to the text by Lee (2018) for a comprehensive treatment. In the following, $\mathcal{L}$ denotes a simply connected smooth manifold modelled on a D-dimensional Hilbert space.

The tangent space at $y \in \mathcal{L}$, denoted by $T_y\mathcal{L}$, is a linear space consisting of velocity vectors $\alpha'(0)$, where $\alpha\colon (-1,1) \to \mathcal{L}$ represents a differentiable curve passing through y, i.e., $\alpha(0) = y$. Each tangent space $T_y\mathcal{L}$ is endowed with an inner product g_y that varies smoothly with y and is a D-dimensional Hilbert space with the induced norm denoted by $\|\cdot\|_y$. The inner products $\{g_y\colon y \in \mathcal{L}\}$ are collectively denoted by g, referred to as the Riemannian metric of $\mathcal{L}$ that also induces a distance d on $\mathcal{L}$.

A geodesic γ is a constant-speed curve defined on $[0,\infty)$ such that, for each $t \in [0,\infty)$, the segment $\gamma([t, t+\epsilon])$ is the shortest path connecting $\gamma(t)$ and $\gamma(t+\epsilon)$ for all sufficiently small $\epsilon > 0$. The Riemannian exponential map Exp_y at $y \in \mathcal{L}$ is a function mapping $T_y\mathcal{L}$ into $\mathcal{L}$ and defined by $\mathrm{Exp}_y(u) = \gamma(1)$ with $\gamma(0) = y$ and $\gamma'(0) = u \in T_y\mathcal{L}$. Conversely, $\gamma_{y,u}(t) = \mathrm{Exp}_y(tu)$ is a geodesic starting at y and with direction u.

For a tangent vector $u \in T_y\mathcal{L}$, the cut time c_u is the positive number such that $\gamma_{y,u}([0,c_u])$ is a shortest path connecting $\gamma_{y,u}(0)$ and $\gamma_{y,u}(c_u)$, but $\gamma_{y,u}([0,c_u+\epsilon])$ is not a shortest path for any $\epsilon > 0$. It turns out that the exponential map $\mathrm{Exp}_y(tu)$ for $u \in T_y\mathcal{L}$ is invertible before the cut time c_u. Formally, the inverse of Exp_y, denoted by Log_y and called the Riemannian logarithmic map at y, can be defined by $\mathrm{Log}_y z = tu$ for $z \in \mathcal{E}_y := \{\mathrm{Exp}_y(tu)\colon u \in T_y\mathcal{L}, \|u\|_y = 1,\ 0 \leqslant t < c_u\}$ such that $\mathrm{Exp}_y(tu) = z$.

Let $C^\infty(\mathcal{L})$ denote the collection of smooth real-valued functions defined on $\mathcal{L}$. For a smooth function $f \in C^\infty(\mathcal{L})$ and a tangent vector $v \in T_y\mathcal{L}$, the covariant derivative of f at y along the direction v, denoted by $\nabla_v f$, is defined by

$$\nabla_v f := (f \circ \gamma)'(0) = \lim_{t\to 0} \frac{f\{\gamma(t)\} - f(y)}{t},$$

where $\gamma\colon [-1,1] \to \mathcal{L}$ is a differentiable curve such that $\gamma(0) = y$ and $\gamma'(0) = v$.

A smooth vector field U is a smooth function defined on $\mathcal{L}$ such that $U(y) \in T_y\mathcal{L}$ for all $y \in \mathcal{L}$. The covariant derivative measures how fast a map changes along a direction and is defined for smooth vector fields as follows. Let $\Gamma(\mathcal{L})$ denote the collection of smooth vector fields on $\mathcal{L}$. A

Downloaded from https://academic.oup.com/biomet/article/110/2/361/6730723 by University of California, Davis - Library user on 04 July 2023

connection is a map $\nabla\colon \Gamma(\mathcal{L}) \times \Gamma(\mathcal{L}) \to \Gamma(\mathcal{L})$, with $(V, U) \mapsto \nabla_V U$, that satisfies the following properties:

(i) $\nabla_V U$ is linear over $C^\infty(\mathcal{L})$ in V, i.e., $\nabla_{fV_1+gV_2}U = f\nabla_{V_1}U + g\nabla_{V_2}U$ for $f, g \in C^\infty(\mathcal{L})$ and $V_1, V_2 \in \Gamma(\mathcal{L})$;
(ii) $\nabla_V U$ is linear over $\mathbb{R}$ in U, i.e., $\nabla_V(a_1U_1 + a_2U_2) = a_1\nabla_V U_1 + a_2\nabla_V U_2$ for $a_1, a_2 \in \mathbb{R}$ and $U_1, U_2 \in \Gamma(\mathcal{L})$;
(iii) $\nabla_V(fU) = f\nabla_V U + (\nabla_V f)U$ for $f \in C^\infty(\mathcal{L})$.

For $f \in C^\infty(\mathcal{L})$ and a smooth vector field U, fU denotes a smooth vector field defined by $(fU)(y) = f(y)U(y)$ for all $y \in \mathcal{L}$, and $\nabla_v f$ is a smooth real-valued function defined by $(\nabla_v f)(y) = \nabla_{V(y)}f$ for $y \in \mathcal{L}$. The quantity $\nabla_V U$ is called the covariant derivative of U in the direction V. The value of $\nabla_V U$ at y depends on V only through its value at y (Proposition 4.5 of Lee, 2018), which makes the expression $\nabla_v U$ sensible for $v \in T_y\mathcal{L}$; $\nabla_v U$ is called the covariant derivative of U at y in the direction v.

For $U, V \in \Gamma(\mathcal{L})$, the function $f_{U,V}$ defined by $f_{U,V}(y) = g_y\{U(y), V(y)\}$ is in $C^\infty(\mathcal{L})$. A connection ∇ on $\mathcal{L}$ is compatible with the metric g on $\mathcal{L}$ if $\nabla_v f_{U,V} = g_y\{\nabla_v U, V(y)\} + g_y\{U(y), \nabla_v V\}$ for all $U, V \in \Gamma(\mathcal{L})$, each $y \in \mathcal{L}$ and each tangent vector $v \in T_y\mathcal{L}$. For $U, V \in \Gamma(\mathcal{L})$, $[U, V]$ denotes a new vector field satisfying $\nabla_{[U,V]}f = \nabla_U\nabla_v f - \nabla_V\nabla_U f$ for all $f \in C^\infty(\mathcal{L})$. If $\nabla_U V - \nabla_V U = [U, V]$ for all $U, V \in \Gamma(\mathcal{L})$, then we say that the connection ∇ is torsion-free. For a Riemannian manifold, there exists a unique connection that is both torsion-free and compatible with the Riemannian metric. It is called the Levi–Civita connection with Levi–Civita covariant derivative as its induced covariant derivative.

Curvature quantifies the degree of deviation from being flat. Define the map $R(U, V, W) = \nabla_U\nabla_V W - \nabla_V\nabla_U W - \nabla_{[U,V]}W$ for $U, V, W \in \Gamma(\mathcal{L})$. The value of $R(U, V, W)$ at y depends only on the values of U, V, W at y, and therefore we can write $R(u, v, w)$ for tangent vectors u, v, w at the same point. The *sectional curvature* at $y \in \mathcal{L}$ is a real-valued function on $T_y\mathcal{L} \times T_y\mathcal{L}$ defined for $u, v \in T_y\mathcal{L}$ by

$$\mathfrak{K}(u, v) = \frac{g_y\{R(u, v, v), u\}}{g_y(u, u)g_y(v, v) - g_y(u, v)^2}.$$

A *Hadamard manifold* is a complete and simply connected Riemannian manifold that has everywhere nonpositive sectional curvature and is thus a Hadamard space.

Given a curve $\gamma(t)$ on $\mathcal{L}$, $t \in I$ for a real interval I, a vector field U along γ is a smooth map defined on I such that $U(t) \in T_{\gamma(t)}\mathcal{L}$. We say that U is parallel along γ if $\nabla_{\gamma'(t)}U = 0$ for all $t \in I$. In this paper, we primarily focus on parallel vector fields along geodesics. Let $\gamma\colon [0, 1] \to \mathcal{L}$ be a geodesic connecting y and z, and let U be a parallel vector field along γ such that $U(0) = u$ and $U(1) = v$. Then we say that v is the parallel transport of u along γ, denoted by $\tau_{y,z}u = v$. Parallel transport can be used as an intrinsic mechanism to compare tangent vectors residing at different points, e.g., via parallelly transporting the tangent vectors to the tangent space at a fixed point on $\mathcal{L}$, where they can be easily compared.

A Lie algebra is a vector space $\mathfrak{g}$ endowed with an alternating binary operation $[\cdot, \cdot]\colon \mathfrak{g} \times \mathfrak{g} \to \mathfrak{g}$ satisfying the following axioms:

(i) (bilinearity) $[au + bv, w] = a[u, w] + b[v, w]$ and $[w, au + bv] = a[w, u] + b[w, v]$ for all $a, b \in \mathbb{R}$ and $u, v, w \in \mathfrak{g}$;
(ii) (alternativity) $[u, u] = 0$ for all $u \in \mathfrak{g}$;
(iii) (Jacobi identity) $[u, [v, w]] + [v, [w, u]] + [w, [u, v]] = 0$ for all $u, v, w \in \mathfrak{g}$.

Downloaded from https://academic.oup.com/biomet/article/110/2/361/6730723 by University of California, Davis - Library user on 04 July 2023

When $\mathcal{L}$ is a group such that the group operation '$\oplus$' and inverse $\iota: y \mapsto y^{-1}$ are smooth, $(\mathcal{L}, \oplus)$ is a Lie group. We say that a vector field U on a Lie group $(\mathcal{L}, \oplus)$ is *left invariant* if $U(y \oplus z) = (D_z L_y)\{U(z)\}$ for all $y, z \in \mathcal{L}$, where $L_y: z \mapsto y \oplus z$ is the left translation induced by y and $D_z L_y$ is the differential of L_y at z. Right-invariant vector fields are defined in a similar fashion via right translations. One can show that any left-invariant vector field U is fully specified by its value $U(e)$ at the group identity element e. Consequently, the collection of left-invariant vector fields, denoted by $\mathfrak{h}$, can be identified with the tangent space $T_e\mathcal{L}$. In addition, the space $\mathfrak{h}$ gives rise to a Lie algebra, as follows. For two smooth vector fields U, V on the Lie group $\mathcal{L}$, the Lie bracket $[U, V]$ is the vector field determined by $[U, V](f) = \nabla_U \nabla_V f - \nabla_V \nabla_U f$ for $f \in C^\infty(\mathcal{L})$. It can be shown that the vector space $\mathfrak{h}$ endowed with the Lie bracket is a Lie algebra. If $\mathcal{L}$ is Abelian then $[U, V] = 0$ for any $U, V \in \mathfrak{h}$.

A Riemannian metric g on a Lie group is left invariant if $g_z(u, v) = g_{y \oplus z}\{(D_z L_y)u, (D_z L_y)v\}$ for all $y, z \in \mathcal{L}$ and $u, v \in T_z\mathcal{L}$. Right-invariant metrics can be defined in a similar fashion. A metric is *bi-invariant* if it is both left invariant and right invariant.

The Lie exponential map, denoted by $\mathfrak{exp}$, that maps $\mathfrak{g}$ into $\mathcal{L}$ is defined by $\mathfrak{exp}(u) = \gamma(1)$, where $\gamma: \mathbb{R} \to \mathcal{L}$ is the unique one-parameter subgroup such that $\gamma'(0) = u \in \mathfrak{g}$. Its inverse, if it exists, is called the Lie logarithmic map and denoted by $\mathfrak{log}$. When g is bi-invariant, $\mathfrak{exp} = \mathrm{Exp}_e$, that is, the Riemannian exponential map at the identity element coincides with the Lie exponential map.

For random elements $Y \in \mathcal{L}$, for a Lie group $\mathcal{L}$, the Fréchet function is $F(y) = \mathbb{E}d^2(y, Y)$, where d is the Riemannian distance function induced by the metric on $\mathcal{L}$. If $\mathcal{L}$ is a Hadamard manifold and $F(y) < \infty$ for some $y \in \mathcal{L}$, and hence $F(y) < \infty$ for all $y \in \mathcal{L}$ according to the triangle inequality, the minimizer of $F(y)$ exists and is unique (Sturm, 2003). It is known as the Fréchet mean and is denoted by $\mathbb{E}_\oplus Y$.

3. Additive models for Lie groups

In this section we develop an additive regression model for Lie group-valued responses. The main motivating example of Lie groups is the space $\mathcal{S}_m^+$ of $m \times m$ symmetric positive matrices due to their ubiquity and practical relevance.

Example 1 ($\mathcal{S}_m^+$ *with the log-Euclidean metric*). The space $\mathcal{S}_m^+$ is a smooth submanifold of $\mathbb{R}^{m \times m}$. Its tangent spaces are $\mathcal{S}_m$, the collection of $m \times m$ symmetric matrices. The matrix logarithm is a smooth bijective map between $\mathcal{S}_m^+$ and $\mathcal{S}_m$, and thus can be used to transfer the canonical Euclidean structure of $\mathcal{S}_m$ to $\mathcal{S}_m^+$. Recall that, for a symmetric matrix S, $\exp(S) = I_m + \sum_{j=1}^\infty S^j/j!$ is a symmetric positive-definite matrix. The inverse of exp, denoted by log, exists and is called the matrix logarithmic map. Both exp and log are smooth maps between $\mathcal{S}_m^+$ and $\mathcal{S}_m$. The operation '$\oplus$' defined as $P_1 \oplus P_2 = \exp\{\log(P_1) + \log(P_2)\}$ for $P_1, P_2 \in \mathcal{S}_m^+$ turns $\mathcal{S}_m^+$ into an Abelian group. The canonical Riemannian metric on $\mathcal{S}_m$ is $\mathrm{trace}(S_1 S_2)$ for $S_1, S_2 \in \mathcal{S}_m$ and can be transferred to a Riemannian metric on $\mathcal{S}_m^+$ given by $g_P(U, V) = \mathrm{trace}[\{(D_P \log)U\}\{(D_P \log)V\}]$ for $U, V \in \mathcal{S}_m$, where $D_P \log$ denotes the differential of the log at P. It turns out that g is a bi-invariant metric on $(\mathcal{S}_m^+, \oplus)$ that is isomorphic to the group of $\mathcal{S}_m$ with the usual matrix addition as the group operation (Proposition 3.4 of Arsigny et al., 2007). This metric, termed the log-Euclidean metric and specifically designed to eliminate the swelling effect (Arsigny et al., 2007), turns $\mathcal{S}_m^+$ into a Hadamard manifold and a bi-invariant Abelian Lie group. This metric is invariant to permutation, but is not affine invariant.

Example 2 ($\mathcal{S}_m^+$ *with the log-Cholesky metric*). The log-Cholesky metric (Lin, 2019) utilizes the Cholesky decomposition to transfer a Lie group structure on the space of lower triangular

Downloaded from https://academic.oup.com/biomet/article/110/2/361/6730723 by University of California, Davis - Library user on 04 July 2023

matrices of positive diagonals to the space of symmetric positive-definitive matrices. Specifically, let $\mathrm{LT}(m)$ be the space of $m \times m$ lower triangular matrices and $\mathrm{LT}_+(m) \subset \mathrm{LT}(m)$ the subspace, such that $L \in \mathrm{LT}_+(m)$ if all diagonal elements of L are positive. One can show that $\mathrm{LT}_+(m)$ is a smooth submanifold of $\mathrm{LT}(m)$ and its tangent spaces are identified with $\mathrm{LT}(m)$. For a fixed $L \in \mathrm{LT}_+(m)$, we define a Riemannian metric $\tilde{g}$ on $\mathrm{LT}_+(m)$ by $\tilde{g}_L(A,B) = \sum_{1 \leqslant j < i \leqslant m} A_{ij}B_{ij} + \sum_{j=1}^{m} A_{jj}B_{jj}L_{jj}^{-2}$, where A_{ij} denotes the element of A in the ith row and jth column. It is an Abelian Lie group with the operation $\circledcirc$ defined by $L_1 \circledcirc L_2 = \mathfrak{L}(L_1) + \mathfrak{L}(L_2) + \mathfrak{D}(L_1)\mathfrak{D}(L_2)$, where $\mathfrak{L}(L)$ is the strict lower triangular part of L, that is, $\{\mathfrak{L}(L)\}_{ij} = L_{ij}$ if $j < i$ and $\{\mathfrak{L}(L)\}_{ij} = 0$ otherwise, and $\mathfrak{D}(L)$ is the diagonal part of L, that is, a diagonal matrix whose diagonals are equal to the respective diagonals of L. One can show that $\tilde{g}$ is a bi-invariant metric for the Lie group $\mathrm{LT}_+(m)$ with the group operation $\circledcirc$. It is well known that a symmetric positive-definite matrix P is associated with a unique matrix L in $\mathrm{LT}_+(m)$ such that $LL^{\mathrm{T}} = P$. We refer to L as the Cholesky factor of P. For $U, V \in T_P\mathcal{S}_m^+ = \mathcal{S}_m$, we define the metric $g_P(U,V) = \tilde{g}_L\{L(L^{-1}UL^{-\mathrm{T}})_{1/2}, L(L^{-1}VL^{-\mathrm{T}})_{1/2}\}$, where $(S)_{1/2} = \mathfrak{L}(S) + \mathfrak{D}(S)/2$ for a matrix S. We also turn $\mathcal{S}_m^+$ into an Abelian Lie group with the operator $\oplus$ such that $P_1 \oplus P_2 = (L_1 \circledcirc L_2)(L_1 \circledcirc L_2)^{\mathrm{T}}$, where L_1 and L_2 are the Cholesky factors of P_1 and P_2, respectively. The metric g, also specifically designed to eliminate the swelling effect (Lin, 2019), is a bi-invariant metric of the Lie group $(\mathcal{S}_m^+, \oplus)$ and turns $\mathcal{S}_m^+$ into a Hadamard manifold. In our experience, the log-Cholesky metric is computationally more efficient, but not invariant to permutation.

The torus serves as an example for a relevant Lie group that is not related to the space $\mathcal{S}_m^+$ and shows that our approach is not limited to symmetric positive matrices.

Example 3 (*Tori*). Let $\mathbb{S} = \{a + b\sqrt{-1} : a, b \in \mathbb{R}, a^2 + b^2 = 1\}$ be the unit circle. It is an Abelian Lie group when the group operation is the standard multiplication of complex numbers. In addition, $\mathbb{S}$ is a Riemannian submanifold of $\mathbb{R}^2$. A k-torus $\mathbb{T}^k$ is the direct product of k copies of $\mathbb{S}$, and is therefore also an Abelian Lie group. Its Lie algebra is $\mathfrak{g} = (-1)^{1/2}\mathbb{R}^k = \{(a_1\sqrt{-1}, \ldots, a_k\sqrt{-1}) : a_1, \ldots, a_k \in \mathbb{R}\}$ with the trivial Lie bracket $[u, v] = 0$ for all $u, v \in \mathfrak{g}$. The Riemannian metric on $\mathbb{T}^k$ is the product Riemannian metric of $\mathbb{S}$, and this metric is bi-invariant. Data on tori occur in the statistical analysis of wind directions and RNA data (Eltzner et al., 2018).

Given scalar variables $X_1 \in \mathcal{X}_1, \ldots, X_q \in \mathcal{X}_q$, which are predictors that are paired with a Lie group-valued response Y and where $\mathcal{X}_j \subset \mathbb{R}$, $j = 1, \ldots q$, are compact domains, the proposed Lie group additive model is as follows, where we make use of the Lie group operation $\oplus$:

$$Y = \mu \oplus w_1(X_1) \oplus \cdots \oplus w_q(X_q) \oplus \zeta. \tag{1}$$

Here $\mu = \mathbb{E}_{\oplus} Y$ is the Fréchet mean of Y, each w_k is a function that maps X_k into $\mathcal{L}$ and ζ is random noise with $\mathbb{E}_{\oplus}\zeta = e$, the group identity element e. For identifiability, we require that $\mathbb{E}_{\oplus}\{w_k(X_k)\} = e$, $k = 1, \ldots, q$. In addition, we assume existence and uniqueness of μ; see § 4 for more discussions. This model generalizes the additive model for Euclidean responses to $\mathcal{L}$-valued responses. It includes the effect of the additive component functions on the mean response and of noise on the responses, neither of which can be additively modelled in the absence of a linear structure of the responses. The task at hand is to estimate the unknown parameter μ and the component functions $w_1, \ldots, w_q$, given a sample of independently and identically distributed observations of size n. To overcome the challenge of the absence of a linear structure in $\mathcal{L}$, the following result proves essential.

Downloaded from https://academic.oup.com/biomet/article/110/2/361/6730723 by University of California, Davis - Library user on 04 July 2023

PROPOSITION 1. *If $(\mathcal{L}, \oplus)$ is an Abelian Lie group endowed with a bi-invariant metric g that turns $\mathcal{L}$ into a Hadamard manifold, then (1) is equivalent to*

$$\mathrm{Log}_\mu Y = \sum_{k=1}^{q} \tau_{e,\mu} \log w_k(X_k) + \tau_{e,\mu} \log \zeta. \tag{2}$$

In (2), we transform the left-hand side of (1) by the Riemannian log map Log_μ, so that $\mathbb{E}\mathrm{Log}_\mu Y = 0$, and the right-hand side of (1) by the Lie log map $\log$, whereupon $w_1(X_1) \oplus \cdots \oplus w_q(X_q)$ is decomposed into additive components in the vector space $T_\mu\mathcal{L}$, so that the standard smooth back-fitting algorithm can be adopted to estimate $w_1, \ldots, w_q$. Specifically, let $f_k(X_k) = \tau_{e,\mu} \log w_k(X_k)$ and $\varepsilon = \tau_{e,\mu} \log \zeta$. Then, according to Proposition 1, one may rewrite model (1) as $\mathrm{Log}_\mu Y = \sum_{k=1}^{q} f_k(X_k) + \varepsilon$, where $\mathbb{E}\varepsilon = \mathbb{E}\tau_{e,\mu} \log \zeta = \tau_{e,\mu} \mathbb{E} \log \zeta = 0$ since $\mathbb{E}_\oplus \zeta = e$. Note that $\mathbb{E}\{\sum_{k=1}^{q} f_k(X_k)\} = 0$ since $\mathbb{E}\mathrm{Log}_\mu Y = 0$. The identifiability of the individual component functions f_k follows from $\mathbb{E}f_k(X_k) = 0$ for all $k = 1, \ldots, q$, which is a consequence of $\mathbb{E}_\oplus\{w_k(X_k)\} = e$ in (1). These considerations motivate us to estimate the component functions w_k through estimation of the f_k, as follows.

Step 1. Compute the sample Fréchet mean $\hat{\mu}$. Closed-form expressions of $\hat{\mu}$ are available for special cases of $\mathcal{L}$, including $\mathcal{L} = \mathcal{S}_m^+$ with the log-Cholesky or log-Euclidean metric; see the Supplementary Material for details. Alternative numerical algorithms (e.g., Yang, 2007) are also available.

Step 2. Compute $\mathrm{Log}_{\hat{\mu}} Y_i$. There are closed-form expressions available for $\mathcal{L} = \mathcal{S}_m^+$ with the log-Cholesky or log-Euclidean metric; see the Supplementary Material. Numerical methods as described in § 5.3 of A. Brun's 2007 PhD thesis from the University of Linköping are also available.

Step 3. Solve the system of integral equations

$$\hat{f}_k(x_k) = \hat{m}_k(x_k) - n^{-1} \sum_{i=1}^{n} \mathrm{Log}_{\hat{\mu}} Y_i - \sum_{j:\, j \neq k} \int_{\mathcal{X}_j} \hat{f}_j(x_j) \frac{\hat{p}_{kj}(x_k, x_j)}{\hat{p}_k(x_k)} \, \mathrm{d}x_j,$$

subject to the constraints $\int_{\mathcal{X}_j} \hat{f}_k(x_k) \hat{p}_k(x_k) \, \mathrm{d}x_k = 0$ for $1 \leqslant k \leqslant q$. Here, $\hat{p}_k(x_k) = n^{-1} \sum_{i=1}^{n} K_{h_k}(x_k, X_{ik})$, $\hat{p}_{kj}(x_k, x_j) = n^{-1} \sum_{i=1}^{n} K_{h_k}(x_k, X_{ik}) K_{h_j}(x_j, X_{ij})$ and

$$\hat{m}_k(x_k) = n^{-1} \hat{p}_k(x_k)^{-1} \sum_{i=1}^{n} K_{h_k}(x_k, X_{ik}) \mathrm{Log}_{\hat{\mu}} Y_i,$$

where K_{h_j} is a kernel function with $\int_{\mathcal{X}_j} K_{h_j}(u, v) \, du = 1$ for all $v \in \mathcal{X}_j$; see Jeon & Park (2020). Note that $n^{-1} \sum_{i=1}^{n} \mathrm{Log}_{\hat{\mu}} Y_i = 0$ since $\hat{\mu}$ is the sample Fréchet mean.

Step 4. Finally, estimate $w_k(x_k)$ by $\hat{w}_k(x_k) = \exp\{\tau_{\hat{\mu},e} \hat{f}_k(x_k)\}$.

Step 3 is a multivariate version of the standard smooth back-fitting system of equations (Mammen et al., 1999). Since the tangent space $T_{\hat{\mu}}\mathcal{L}$ is also a Hilbert space, the above smooth back-fitting system of equations can be interpreted from a Bochner integral perspective; see Jeon & Park (2020), where also the empirical selection of bandwidths h_k is discussed.

Downloaded from https://academic.oup.com/biomet/article/110/2/361/6730723 by University of California, Davis - Library user on 04 July 2023

Remark 1. By Theorem 3.6 of Bröcker & tom Dieck (1985), any Abelian Lie group is isomorphic to $\mathbb{T}^k \times \mathbb{R}^s$, where $\mathbb{T}^k$ denotes a k-torus defined in Example 3. However, our model, estimation and theory do not rest on this isomorphism, as it does not lead to a natural extension to general Riemannian manifolds. Instead, in the above development we connect the additive model (1) on Lie groups to an additive model (2) on the tangent space at the Fréchet mean via Proposition 1. This allows an immediate extension to general Riemannian manifolds. Since neither our estimation method nor the theory presented in § 5 relies on the isomorphism to $\mathbb{T}^k \times \mathbb{R}^s$, our methods and theory cover both Lie groups and general Riemannian manifolds.

4. EXTENSION TO RIEMANNIAN MANIFOLDS

When $\mathcal{S}_m^+$ is endowed with the affine-invariant metric (Moakher, 2005; Pennec et al., 2006; Fletcher & Joshib, 2007), it is generally not an Abelian Lie group with a bi-invariant metric, and then model (1) depends on the order of operations and is thus not additive. Specifically, Proposition 1 ceases to hold. However, model (2) remains additive in all cases, suggesting a natural extension to accommodate other metrics and general Riemannian manifolds. For a Riemannian manifold $\mathcal{M}$, which is not necessarily an Abelian Lie group, consider

$$\mathrm{Log}_\mu Y = \sum_{k=1}^{q} f_k(X_k) + \varepsilon, \tag{3}$$

where $\mu = \mathbb{E}_\oplus Y$, $\varepsilon \in T_\mu\mathcal{M}$ is centred and of finite variance, and $f_1, \ldots, f_q \colon \mathbb{R} \to T_\mu\mathcal{M}$ are unknown functions to be estimated. Model (3) includes (1) as a special case by setting $f_k(x) = \tau_{e,\mu}\log w_k(x)$ and $\varepsilon = \tau_{e,\mu}\log\zeta$ according to Proposition 1, transforms the response into the tangent space $T_\mu\mathcal{M}$ and is thus applicable to general Riemannian manifolds, at the expense of interpretability in the original space, as per the group operation in model (1).

For general Riemannian manifolds that might feature positive sectional curvature, the Fréchet mean may not exist and therefore additional conditions are required for model (3). Specifically, if $(\mathcal{M}, g)$ is a general Riemannian manifold and Y is a random element on $\mathcal{M}$, we assume the following.

Assumption 1. The minimizer of the Fréchet function $F(\cdot) = \mathbb{E}d^2(\cdot, Y)$ exists and is unique.

This is automatically satisfied when $\mathcal{M}$ is a Hadamard manifold, such as the space $\mathcal{S}_m^+$ with either of the log-Cholesky and log-Euclidean metrics. For other manifolds, we refer the reader to Bhattacharya & Patrangenaru (2003) and Afsari (2011) for conditions that imply Assumption 1.

For a nonempty subset $A \subset \mathcal{M}$, let $d(y, A) = \inf\{d(y, z) : z \in A\}$ denote the distance between y and the set A. For a positive real number ϵ, set $A^\epsilon = \{y : d(y, A) < \epsilon\}$ and $A^{-\epsilon} = \mathcal{M}\backslash(\mathcal{M}\backslash A)^\epsilon$. When $A = \emptyset$, set $A^\epsilon = \emptyset$. The following assumption is only needed for the case where $\mathcal{M}$ is not a Hadamard manifold.

Assumption 2. It holds that $\Pr\{Y \in \mathcal{E}_\mu^{-\epsilon_0}\} = 1$ for some $\epsilon_0 > 0$, where $\mathcal{E}_\mu$ is defined in § 2.

If Assumptions 1 and 2 are satisfied, the proposed manifold additive model (3) remains well defined, and the first three steps of the estimation method described in the previous section are still valid and can be employed to estimate $f_1, \ldots, f_q$, with $\mathcal{L}$ replaced by $\mathcal{M}$.

Downloaded from https://academic.oup.com/biomet/article/110/2/361/6730723 by University of California, Davis - Library user on 04 July 2023

5. Theory

We first establish convergence rates and asymptotic normality of the estimators for the mean and the component functions for general manifolds in the manifold additive model (3), and then provide additional details for the space $\mathcal{S}_m^+$ endowed with either the log-Cholesky metric or the log-Euclidean metric. We consider a manifold $\mathcal{M}$ that satisfies one of the following conditions.

Condition 1. Manifold $\mathcal{M}$ is a finite-dimensional Hadamard manifold that has sectional curvature bounded from below by $\mathfrak{c}_0 \leqslant 0$.

Condition 2. Manifold $\mathcal{M}$ is a complete compact Riemannian manifold.

An example of a manifold satisfying Condition 1 is $\mathcal{S}_m^+$ endowed with the log-Cholesky metric, log-Euclidean metric or affine-invariant metric, while the unit sphere that is used to model compositional data (Dai & Müller, 2018) serves as an example of a manifold that satisfies Condition 2.

To establish the convergence rate of $\hat{\mu}$, we also make the following assumptions.

Assumption 3. Manifold $\mathcal{M}$ satisfies at least one of Conditions 1 and 2.

Assumption 4. For some constant $\mathfrak{c}_2 > 0$, $F(y) - F(\mu) \geqslant \mathfrak{c}_2 d^2(y, \mu)$ when $d(y, \mu)$ is sufficiently small.

Assumption 5. For some constant $\mathfrak{c}_3 > 0$, for all $y, z \in \mathcal{M}$, the linear operator $H_{y,z} : T_z\mathcal{M} \to T_z\mathcal{M}$, defined by $g_z(H_{y,z}u, v) = g_z(\nabla_u \mathrm{Log}_z y, v)$ for $u, v \in T_z\mathcal{M}$, has an operator norm that is bounded by $\mathfrak{c}_3\{1 + d(z, y)\}$.

Assumption 4 is satisfied for Hadamard manifolds with $\mathfrak{c}_2 = 1$ according to Lemma S.7 of Lin & Müller (2021), and the CAT(0) inequality that holds for Hadamard manifolds (Chapter II.1 of Bridson & Häfliger, 1999). The assumption also holds for some manifolds of positive curvature when data concentrate on a small region; see Example 4 of Lin & Müller (2021). The operator $H_{y,z}$ in the technical Assumption 5 is the Hessian of the squared distance function d; see also equation (5.4) of Kendall & Le (2011). Assumption 5 is superfluous if the manifold $\mathcal{M}$ is compact and is satisfied by manifolds of zero curvature. It can also be replaced with a uniform moment condition on the operator norm of $H_{z,Y}$ over all z in a small local neighbourhood of μ. We then obtain a parametric convergence rate for the estimate $\hat{\mu}$ of the Fréchet mean μ.

Proposition 2. *Assume that Assumptions 1, 3 and 4 hold and that Y is of second order. Then* $d(\hat{\mu}, \mu) = O_P(n^{-1/2})$.

To obtain convergence rates of the estimated component functions, we require some additional conditions that are standard in the literature on additive regression.

Condition 3. The kernel function K is positive, symmetric, Lipschitz continuous and supported on $[-1, 1]$ with $\int K(x)\,dx = 1$.

Condition 4. The bandwidths h_k satisfy $n^{1/5}h_k \to \alpha_k > 0$.

Condition 5. The joint density p of $X_1, \ldots, X_q$ is bounded away from zero and infinity on $\mathcal{X} \equiv \mathcal{X}_1 \times \cdots \times \mathcal{X}_q$. The densities p_{kj} are continuously differentiable for $1 \leqslant j \neq k \leqslant q$.

Downloaded from https://academic.oup.com/biomet/article/110/2/361/6730723 by University of California, Davis - Library user on 04 July 2023

Condition 6. The additive functions f_k are twice continuously (Fréchet) differentiable.

Without loss of generality, assume that $\mathcal{X}_k = [0,1]$ for all k and let $\mathcal{I}_k = [2h_k, 1-2h_k]$. The moment condition on ε in the following theorem is required to control the effect of the error of $\hat{\mu}$ as an estimator of μ on the discrepancies of $\mathrm{Log}_{\hat{\mu}} Y_i$ from $\mathrm{Log}_{\mu} Y_i$ after parallel transport; see the Supplementary Material. It is a mild requirement and is satisfied for example when the manifold is compact or $\|\varepsilon\|_\mu$ follows a subexponential distribution.

THEOREM 1. *Under Assumptions 1–5 and Conditions 3–6, if* $\mathbb{E}\|\varepsilon\|_\mu^\alpha < \infty$ *for some* $\alpha \geqslant 10$ *and* $\mathbb{E}(\|\varepsilon\|_\mu^2 \mid X_j = \cdot)$ *are bounded on* $\mathcal{X}_j$*, respectively, for* $1 \leqslant j \leqslant q$*, it holds that*

$$\max_{1\leqslant k\leqslant q} \int_{\mathcal{I}_k} \|\tau_{\hat{\mu},\mu}\hat{f}_k(x_k) - f_k(x_k)\|_\mu^2 \, p_k(x_k)\,\mathrm{d}x_k = O_P(n^{-4/5}),$$

$$\max_{1\leqslant k\leqslant q} \int_{\mathcal{X}_k} \|\tau_{\hat{\mu},\mu}\hat{f}_k(x_k) - f_k(x_k)\|_\mu^2 \, p_k(x_k)\,\mathrm{d}x_k = O_P(n^{-3/5}),$$

where $\tau_{\hat{\mu},\mu}$ *is the parallel transport operator along geodesics.*

The following corollary is an immediate consequence of Theorem 1.

COROLLARY 1. *Under the conditions of Theorem 1, for* $\mathcal{S}_m^+$ *endowed with either the log-Cholesky metric or the log-Euclidean metric,*

$$\max_{1\leqslant k\leqslant q} \int_{\mathcal{I}_k} \|\log\hat{w}_k(x_k) - \log w_k(x_k)\|_e^2 \, p_k(x_k)\,\mathrm{d}x_k = O_P(n^{-4/5}),$$

$$\max_{1\leqslant k\leqslant q} \int_{\mathcal{X}_k} \|\log\hat{w}_k(x_k) - \log w_k(x_k)\|_e^2 \, p_k(x_k)\,\mathrm{d}x_k = O_P(n^{-3/5}).$$

To derive the asymptotic distribution of $\hat{f}_k$, we define $\mathscr{C}_k(x) = \mathbb{E}\{\varepsilon \otimes \varepsilon \mid X_k = x\}$, where $u \otimes v \colon T_\mu\mathcal{M} \to T_\mu\mathcal{M}$ is a tensor product operator such that $(u \otimes v)z = g_\mu(u,z)v$. Define

$$\Sigma_k(x) = \alpha_k^{-1} p_k(x)^{-1} \int K(u)^2 \,\mathrm{d}u \cdot \mathscr{C}_k(x), \tag{4}$$

$$\delta_k(x) = \frac{p_k'(x)}{p_k(x)} \int u^2 K(u)\ \mathrm{d}u \cdot f_k'(x), \tag{5}$$

$$\delta_{jk}(x,v) = \frac{\partial p_{jk}(x,v)}{\partial v} \frac{1}{p_{jk}(x,v)} \int u^2 K(u)\ \mathrm{d}u \cdot f_k'(v), \tag{6}$$

$$\tilde{\Delta}_k(x) = \alpha_k^2 \cdot \delta_k(x) + \sum_{j:j\neq k} \alpha_j^2 \int_{\mathcal{X}_j} \frac{p_{kj}(x,u)}{p_k(x)} \cdot \delta_{kj}(x,u)\ \mathrm{d}u, \tag{7}$$

where the α_k are the constants in Condition 4. Let $(\Delta_1, \ldots, \Delta_q)$ be a solution of the system of equations

$$\Delta_k(x) = \tilde{\Delta}_k(x) - \sum_{j:j\neq k} \int_{\mathcal{X}_j} \frac{p_{kj}(x,u)}{p_k(x)} \cdot \Delta_j(u)\,\mathrm{d}u, \qquad 1 \leqslant k \leqslant q, \tag{8}$$

Downloaded from https://academic.oup.com/biomet/article/110/2/361/6730723 by University of California, Davis - Library user on 04 July 2023

satisfying the constraints

$$\int_{\mathcal{X}_k} p_k(x) \cdot \Delta_k(x)\,\mathrm{d}x = \alpha_k^2 \cdot \int_{\mathcal{X}_k} p_k(x) \cdot \delta_k(x)\,\mathrm{d}x, \qquad 1 \leqslant k \leqslant q. \tag{9}$$

Finally, define $c_k(x) = \frac{1}{2}\int u^2 K(u)\ \mathrm{d}u \cdot f_k''(x)$ and $\theta_k(x) = \alpha_k^2 \cdot c_k(x) + \Delta_k(x)$.

We assume that the following conditions hold.

Condition 7. The $\mathbb{E}\{\varepsilon \otimes \varepsilon \mid X_k = \cdot\}$ are continuous operators on $\mathcal{X}_k$ for all $1 \leqslant k \leqslant q$ and operators $\mathbb{E}\{\varepsilon \otimes \varepsilon \mid X_j = \cdot, X_k = \cdot\}$ are bounded on $\mathcal{X}_j \times \mathcal{X}_k$ for all $1 \leqslant j \neq k \leqslant q$.

Condition 8. The $\partial p/\partial x_k$, $k = 1, \ldots, q$, exist and are bounded on $\mathcal{X} = \prod_{k=1}^q \mathcal{X}_k$.

Condition 7 is superfluous if the random noise ε is independent of the predictors $X_1, \ldots, X_q$. Let $N_\mu(\boldsymbol{x})$ be the product measure $N\{\theta_1(x_1), \Sigma_1(x_1)\} \times \cdots \times N\{\theta_q(x_q), \Sigma_q(x_q)\}$ on $(T_\mu\mathcal{M})^q$, where $N(\theta, \Sigma)$ denotes a Gaussian measure on $T_\mu\mathcal{M}$ with mean vector θ and covariance operator Σ. For a set A, let $\mathrm{Int}(A)$ denote the interior of A.

THEOREM 2. *Suppose that Assumptions 1–5 and Conditions 3–8 hold, that* $\mathbb{E}\|\varepsilon\|_\mu^\alpha < \infty$ *for some* $\alpha > 10$ *and that there exists* $\alpha' > 5/2$ *such that* $\mathbb{E}(\|\varepsilon\|_\mu^{\alpha'} \mid X_k = \cdot)$ *are bounded on* $\mathcal{X}_k$ *for all* $1 \leqslant k \leqslant q$. *Then, for* $\boldsymbol{x} = (x_1, \ldots, x_q) \in \mathrm{Int}(\mathcal{X})$, *it holds that* $[n^{2/5}\{\tau_{\hat{\mu},\mu}\hat{f}_k(x_k) - f_k(x_k)\} : 1 \leqslant k \leqslant q] \to N_\mu(\boldsymbol{x})$ *in distribution. In addition,* $n^{2/5}\{\sum_{k=1}^q \tau_{\hat{\mu},\mu}\hat{f}_k(x_k) - \sum_{k=1}^q f_k(x_k)\}$ *converges to* $N_\mu\{\theta(\boldsymbol{x}), \Sigma(\boldsymbol{x})\}$, *where* $\theta(\boldsymbol{x}) = \sum_{k=1}^q \theta_k(x_k)$ *and* $\Sigma(\boldsymbol{x}) = \Sigma_1(x_1) + \cdots + \Sigma_q(x_q)$.

For $\mathcal{M} = \mathcal{S}_m^+$ equipped with either the log-Cholesky metric or the log-Euclidean metric, the above asymptotic normality can be formulated on the Lie algebra $\mathfrak{g}$. To this end, assume that $\Sigma_1^{\mathrm{SPD}}, \ldots, \Sigma_q^{\mathrm{SPD}}$ and $\Delta_1^{\mathrm{SPD}}, \ldots, \Delta_q^{\mathrm{SPD}}$ are defined by (4)–(9), with $\mathscr{C}_k(x)$ and f_k replaced by $\mathbb{E}\{\log\zeta \otimes \log\zeta \mid X_k = x\}$ and $\psi_k := \log w_k$, respectively. Also, let $c_k^{\mathrm{SPD}} = \frac{1}{2}\int u^2 K(u)\ \mathrm{d}u \cdot \psi_k''(x)$ and $\theta_k^{\mathrm{SPD}}(x) = \alpha_k^2 \cdot c_k^{\mathrm{SPD}}(x) + \Delta_k^{\mathrm{SPD}}(x)$ for $k = 1, \ldots, q$. The following corollary is an immediate consequence of Theorem 2, by noting that the manifold $\mathcal{S}_m^+$ when equipped with the log-Cholesky metric or the log-Euclidean metric satisfies Assumptions 1–4 when the second moment of the random noise ζ is finite.

COROLLARY 2. *Assume that Conditions 3–8 hold and that* $\mathbb{E}\|\log\zeta\|_\mu^\alpha < \infty$ *for some* $\alpha > 10$. *Furthermore, assume that there exists* $\alpha' > 5/2$ *such that* $\mathbb{E}(\|\log\zeta\|_e^{\alpha'} \mid X_k = \cdot)$ *are bounded on* $\mathcal{X}_k$ *for all* $1 \leqslant k \leqslant q$. *For* $\mathcal{S}_m^+$ *endowed with either the log-Cholesky metric or the log-Euclidean metric, for* $\boldsymbol{x} = (x_1, \ldots, x_q) \in \mathrm{Int}(\mathcal{X})$, *it holds that* $[n^{2/5}\{\log\hat{w}_k(x_k) - \log w_k(x_k)\} : 1 \leqslant k \leqslant q] \to N_{I_m}(\boldsymbol{x})$ *in distribution. In addition,* $n^{2/5}\{\sum_{k=1}^q \log\hat{w}_k(x_k) - \sum_{k=1}^q \log w_k(x_k)\}$ *converges to* $N_{I_m}\{\theta(\boldsymbol{x}), \Sigma(\boldsymbol{x})\}$, *where* I_m *is the* $m \times m$ *identity matrix,* $\theta(\boldsymbol{x}) = \sum_{k=1}^q \theta_k^{\mathrm{SPD}}(x_k)$ *and* $\Sigma(\boldsymbol{x}) = \Sigma_1^{\mathrm{SPD}}(x_q) + \cdots + \Sigma_q^{\mathrm{SPD}}(x_q)$.

These results generalize the work of Jeon & Park (2020). One of the major technical challenges that is addressed in Lemmas S1 and S2 in the Supplementary Material is to uniformly quantify the discrepancy between $\log_{\hat{\mu}} Y_i$ and $\log_\mu Y_i$ due to $\hat{\mu} \neq \mu$, as the asymptotic behaviour of this discrepancy plays an important role in the theoretical analysis.

Downloaded from https://academic.oup.com/biomet/article/110/2/361/6730723 by University of California, Davis - Library user on 04 July 2023

6. SIMULATIONS

To illustrate the numerical performance of the proposed manifold additive model estimators, we conducted simulations for $\mathcal{L} = \mathcal{S}_m^+$ endowed with the log-Cholesky and log-Euclidean metrics, respectively. We consider two matrix dimensions, $m = 3$ and $m = 10$. We set $\mathcal{X}_k = [0, 1]$ for $k = 1, \ldots, q$. The predictors $X_1, \ldots, X_q$ are set to $X_1 = B_{2/3,2/3}(T_1)$ and $X_k = \Phi(T_k)$ for $k = 2, \ldots, q$, where $B_{2/3,2/3}$ denotes the cumulative distribution function of the beta distribution with both shape parameters equal to $2/3$, Φ denotes the cumulative distribution function of the standard Gaussian distribution, and $(T_1, \ldots, T_q)$ is sampled from the centred q-dimensional Gaussian distribution with covariance matrix whose (j, k)th entry is 1 if $j = k$ and $1/5$ if $j \neq k$. Consequently, $X_1, \ldots, X_q$ are correlated and X_1 has a nonuniform distribution on $[0, 1]$. The mean μ is an $m \times m$ matrix whose (j, k)th entry is $2^{-|j-k|}$. We then generate the response variable Y by $Y = \mu \oplus w(X_1, \ldots, X_q) \oplus \zeta$, where $w(X_1, \ldots, X_q) = \exp_\mu \tau_{\mu,e} f(X_1, \ldots, X_q)$ with three settings for f:

I. $f(x_1, \ldots, x_q) = \sum_{k=1}^q f_k(x_k)$ with $f_k(x_k)$ being an $m \times m$ matrix whose (j, l)th entry is $g(x_k; j, l, q) = \exp(-|j - l|/q) \sin[2q\pi\{x_k - (j + l)/q\}]$;
II. $f(x_1, \ldots, x_q) = f_{12}(x_1, x_2) + \sum_{k=3}^q f_k(x_k)$, where f_k is defined as in setting I, while $f_{12}(x_1, x_2)$ is an $m \times m$ matrix whose (j, l)th entry is $g(x_1; j, l, q)g(x_2, j, l, q)$;
III. $f(x_1, \ldots, x_q) = f_{12}(x_1, x_2) \prod_{k=3}^q f_k(x_k)$, where $f_{12}(x_1, x_2)$ is an $m \times m$ matrix whose (j, l)th entry is $\exp\{-(j + l)(x_1 + x_2)\}/3$, and $f_k(x_k)$ is an $m \times m$ matrix whose (j, l)th entry is $\sin(2\pi x_k)$.

The random noise ζ is generated according to $\log \zeta = \sum_{j=1}^p Z_j v_j$, where $p = m(m + 1)/2$ is the dimension of $T_e\mathcal{S}_m^+$, $Z_1, \ldots, Z_p$ are independently sampled from $N(0, \sigma^2)$ and $v_1, \ldots, v_p$ form an orthonormal basis of the tangent space $T_e\mathcal{S}_m^+$. The signal-to-noise ratio is measured by $\text{SNR} = \mathbb{E}\|\log w(X_1, \ldots, X_q)\|_e^2 / \mathbb{E}\|\log \zeta\|_e^2$. We tweak the value of the parameter σ^2 to cover two settings for the signal-to-noise ratio, namely, $\text{SNR} = 2$ and $\text{SNR} = 4$. Model I is additive, while models II and III are not additive. In particular, model III has no additive components and thus represents the most challenging scenario for the proposed additive regression. We consider $q = 3$ and $q = 4$ to probe the effect of the dimensionality of the predictor vector and study sample sizes $n = 50, 100, 200$.

The quality of the estimation is measured by the root-mean-square error

$$\text{RMSE} = \left[\int_{[0,1]^q} d^2\{\hat{\mu} \oplus \hat{w}_1(x_1) \oplus \cdots \oplus \hat{w}_q(x_q), f(x_1, \ldots, x_q)\} \, \mathrm{d}x_1 \cdots \mathrm{d}x_q \right]^{1/2}.$$

As a comparison method for the proposed manifold additive model, we also implemented the intrinsic local polynomial regression proposed in Yuan et al. (2012), which is a fully nonparametric approach. In addition, we implemented the following baseline method proposed by an anonymous reviewer, which provides a simple and straightforward approach based on Cholesky decomposition: each symmetric positive-definite matrix is represented by its Cholesky factor, and then a standard multivariate additive model is applied for the Cholesky factor. This simple method may be subject to the swelling effect as it does not use a swelling-free geometry on $\mathcal{S}_m^+$; see Example 1 of Lin (2019) for an illustration. Each simulation setting was repeated 100 times. The Monte Carlo prediction root-mean-square error and its standard error are shown in Table 1 for the log-Cholesky metric and in Table 2 for the log-Euclidean metric for $m = 3$; the results for $m = 10$ are similar and can be found in the Supplementary Material, where we also graphically

Downloaded from https://academic.oup.com/biomet/article/110/2/361/6730723 by University of California, Davis - Library user on 04 July 2023

Table 1. *Prediction* RMSE *and its Monte Carlo standard error with* $m = 3$ *(log Cholesky)*

Setting	q	n	MAM		ILPR		CHOL	
			SNR $= 2$	SNR $= 4$	SNR $= 2$	SNR $= 4$	SNR $= 2$	SNR $= 4$
I	3	50	1.046 (0.093)	0.967 (0.092)	1.604 (0.105)	1.546 (0.233)	1.376 (0.112)	1.329 (0.120)
		100	0.695 (0.049)	0.624 (0.040)	1.528 (0.127)	1.452 (0.218)	1.248 (0.108)	1.171 (0.123)
		200	0.541 (0.040)	0.412 (0.038)	1.392 (0.110)	1.320 (0.151)	1.200 (0.109)	1.187 (0.117)
	4	50	1.665 (0.082)	1.458 (0.154)	1.865 (0.065)	1.871 (0.170)	1.931 (0.096)	1.890 (0.074)
		100	1.087 (0.049)	0.965 (0.065)	1.786 (0.033)	1.759 (0.028)	1.829 (0.134)	1.678 (0.045)
		200	0.754 (0.073)	0.608 (0.050)	1.743 (0.029)	1.726 (0.033)	1.683 (0.087)	1.616 (0.050)
II	3	50	1.121 (0.045)	1.073 (0.063)	1.399 (0.161)	1.195 (0.128)	1.186 (0.064)	1.156 (0.052)
		100	0.910 (0.045)	0.822 (0.037)	1.191 (0.131)	1.125 (0.103)	1.016 (0.085)	0.915 (0.055)
		200	0.774 (0.042)	0.711 (0.025)	1.151 (0.122)	1.093 (0.126)	0.861 (0.043)	0.782 (0.026)
	4	50	1.495 (0.037)	1.463 (0.049)	1.601 (0.075)	1.644 (0.117)	1.654 (0.076)	1.582 (0.070)
		100	1.203 (0.064)	1.117 (0.099)	1.521 (0.025)	1.507 (0.021)	1.569 (0.094)	1.451 (0.062)
		200	0.916 (0.051)	0.817 (0.043)	1.481 (0.022)	1.469 (0.020)	1.396 (0.103)	1.350 (0.103)
III	3	50	0.640 (0.054)	0.629 (0.055)	0.713 (0.107)	0.696 (0.101)	0.593 (0.053)	0.609 (0.050)
		100	0.574 (0.041)	0.555 (0.050)	0.678 (0.051)	0.616 (0.077)	0.559 (0.042)	0.547 (0.063)
		200	0.530 (0.043)	0.515 (0.045)	0.637 (0.084)	0.589 (0.067)	0.535 (0.037)	0.526 (0.051)
	4	50	0.603 (0.059)	0.551 (0.036)	0.647 (0.068)	0.624 (0.097)	0.602 (0.055)	0.597 (0.036)
		100	0.584 (0.048)	0.549 (0.046)	0.616 (0.092)	0.617 (0.054)	0.573 (0.041)	0.576 (0.045)
		200	0.540 (0.063)	0.521 (0.039)	0.586 (0.058)	0.583 (0.037)	0.584 (0.061)	0.566 (0.038)

MAM, the proposed manifold additive model; ILPR, intrinsic local polynomial regression proposed in Yuan et al. (2012); CHOL, a baseline method based on Cholesky decomposition; SNR, signal-to-noise ratio.

Table 2. *Prediction* RMSE *and its Monte Carlo standard error with* $m = 3$ *(log Euclidean)*

Setting	q	n	MAM		ILPR		CHOL	
			SNR $= 2$	SNR $= 4$	SNR $= 2$	SNR $= 4$	SNR $= 2$	SNR $= 4$
I	3	50	2.452 (0.258)	2.122 (0.218)	3.450 (0.396)	3.121 (0.351)	3.441 (0.323)	3.129 (0.301)
		100	1.576 (0.094)	1.305 (0.127)	3.135 (0.240)	3.120 (0.217)	3.034 (0.218)	2.890 (0.260)
		200	1.217 (0.067)	0.914 (0.060)	3.025 (0.109)	2.945 (0.190)	2.922 (0.172)	2.823 (0.223)
	4	50	3.573 (0.182)	3.355 (0.350)	3.949 (0.205)	3.879 (0.132)	4.478 (0.299)	4.388 (0.223)
		100	2.436 (0.201)	2.079 (0.163)	3.712 (0.196)	3.680 (0.184)	4.173 (0.224)	4.059 (0.276)
		200	1.802 (0.176)	1.333 (0.120)	3.621 (0.152)	3.603 (0.137)	4.015 (0.231)	3.701 (0.274)
II	3	50	2.418 (0.107)	2.239 (0.120)	2.736 (0.259)	2.517 (0.126)	2.756 (0.175)	2.467 (0.112)
		100	1.960 (0.149)	1.750 (0.077)	2.493 (0.290)	2.480 (0.301)	2.491 (0.183)	2.140 (0.155)
		200	1.665 (0.083)	1.563 (0.051)	2.440 (0.311)	2.411 (0.223)	1.954 (0.112)	1.782 (0.062)
	4	50	3.292 (0.341)	3.150 (0.254)	3.396 (0.266)	3.412 (0.276)	3.693 (0.245)	3.654 (0.289)
		100	2.769 (0.286)	2.442 (0.108)	3.215 (0.286)	3.201 (0.251)	3.475 (0.250)	3.424 (0.189)
		200	2.151 (0.102)	1.872 (0.073)	3.149 (0.230)	3.130 (0.235)	3.289 (0.279)	3.207 (0.308)
III	3	50	0.850 (0.030)	0.937 (0.138)	1.093 (0.080)	0.922 (0.063)	0.875 (0.042)	0.833 (0.059)
		100	0.801 (0.050)	0.762 (0.042)	0.895 (0.055)	0.813 (0.074)	0.875 (0.165)	0.823 (0.060)
		200	0.706 (0.048)	0.674 (0.063)	0.829 (0.033)	0.801 (0.037)	0.773 (0.067)	0.753 (0.074)
	4	50	0.853 (0.066)	0.832 (0.058)	1.002 (0.074)	0.902 (0.062)	0.889 (0.077)	0.872 (0.096)
		100	0.837 (0.044)	0.832 (0.039)	0.890 (0.066)	0.845 (0.071)	0.871 (0.058)	0.855 (0.057)
		200	0.815 (0.059)	0.802 (0.032)	0.844 (0.056)	0.810 (0.052)	0.860 (0.088)	0.839 (0.043)

MAM, the proposed manifold additive model; ILPR, intrinsic local polynomial regression proposed in Yuan et al. (2012); CHOL, a baseline method based on Cholesky decomposition; SNR, signal-to-noise ratio.

illustrate the estimation quality of the proposed method for SNR $= 4$, $q = 3$, $m = 3$ and the log-Euclidean metric.

When the model is correctly specified as in setting I, the proposed model outperforms the other two methods by a significant margin. When the underlying model is not fully additive, but

Downloaded from https://academic.oup.com/biomet/article/110/2/361/6730723 by University of California, Davis - Library user on 04 July 2023

contains some additive components, such as the model in setting II, our proposed approach still outperforms the other two methods. When the true model has no additive components, such as the model in setting III, all methods have comparable performance when data are sampled from the log-Cholesky metric, while our method and the Cholesky-based method exhibit advantages for the log-Euclidean metric. Also, our method enjoys smaller prediction root mean squared error, compared to the baseline Cholesky method in settings I and II, while both have similar prediction root-mean-square error in setting III. As the true model is unknown in reality and our method is competitive even when there are no additive components, our proposed manifold additive model is overall preferable in applications. In terms of computational efficiency, we found that the log-Cholesky metric is computationally faster than the log-Euclidean metric. In addition, the proposed method for the log-Cholesky metric and the baseline method have comparable computational efficiency, while intrinsic local polynomial regression is fastest in computation; see the Supplementary Material.

7. APPLICATION TO DIFFUSION TENSOR IMAGING

We applied the proposed additive model to diffusion tensors obtained from the Alzheimer's Disease Neuroimaging Initiative, ADNI. Diffusion tensors are 3×3 symmetric positive-definite matrices that characterize diffusion of water molecules in tissues, and convey rich information about brain tissues with important applications in tractography. They are utilized to aid in the diagnosis of brain-related diseases. In statistical modelling, diffusion tensors are typically considered to be random elements in the space $\mathcal{S}_3^+$ (Fillard et al., 2005; Arsigny et al., 2006; Lenglet et al., 2006; Pennec, 2006; Fletcher & Joshib, 2007; Dryden et al., 2009; Zhu et al., 2009; Zhou et al., 2016; Pennec, 2020). A traditional Euclidean framework for diffusion tensors suffers from significant swelling effects that undesirably inflate the diffusion tensors (Arsigny et al., 2007) and impede their interpretation. In our analysis we use diffusion tensors as responses under the log-Euclidean metric, which is designed to eliminate the swelling effect and relate these responses to several covariates.

We focus on the hippocampus, which plays a central role in Alzheimer's disease (Lindberg et al., 2012). In the ADNI study, brain images and assessment of memory, executive functioning and language ability were obtained for participating subjects. For each raw diffusion tensor image, a standard pre-processing protocol including denoising, eddy current and motion correction, skull stripping, bias correction and normalization was applied and then diffusion tensors for each hippocampal voxel were extracted, followed by computing their log-Euclidean mean. For each raw image, this resulted in an average diffusion tensor representing the typical hippocampal diffusion of the corresponding subject at the time of visit. To study the relation between the average hippocampal diffusion tensor and memory, executive functioning and language ability of the subject, we utilized the neuropsychological summary scores available from ADNI (Gibbons et al., 2012). We only included data from the first visit of subjects who were diagnosed as having either early mild cognitive impairment, mild cognitive impairment, late mild cognitive impairment or Alzheimer's disease. Records with missing values were excluded, under the assumption that missingness occurs at random. This resulted in 220 data tuples of the form (Y, X_1, X_2, X_3), where Y is the average diffusion tensor, which serves as response, while the predictors X_1, X_2, X_3 are standardized scores for memory, executive functioning and language ability, respectively. A subset of the data is presented in Fig. 1.

The estimated component functions $\hat{w}_1(x_1), \hat{w}_2(x_2), \hat{w}_3(x_3)$ and their individual effect on the diffusion tensors are depicted in Fig. 2. For interpretation, we denote the coordinate system of

Downloaded from https://academic.oup.com/biomet/article/110/2/361/6730723 by University of California, Davis - Library user on 04 July 2023

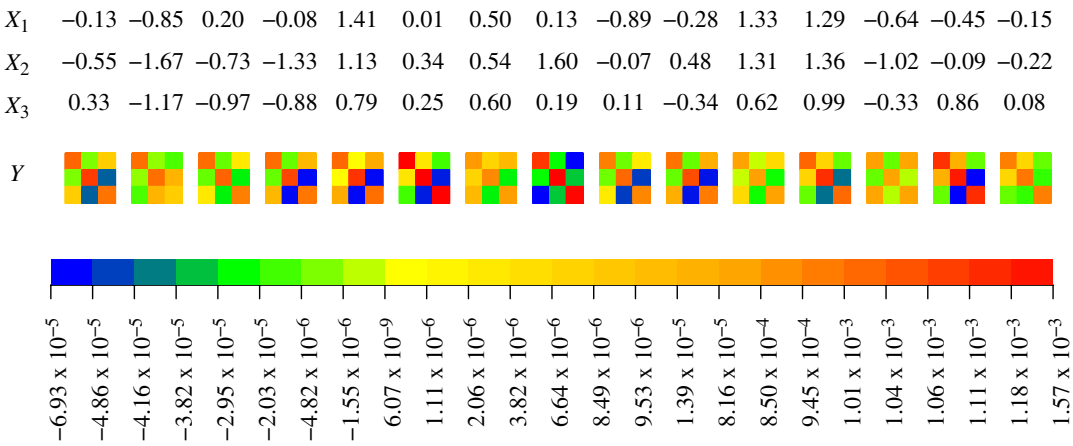

Fig. 1. A random sample of 15 observations from the data.

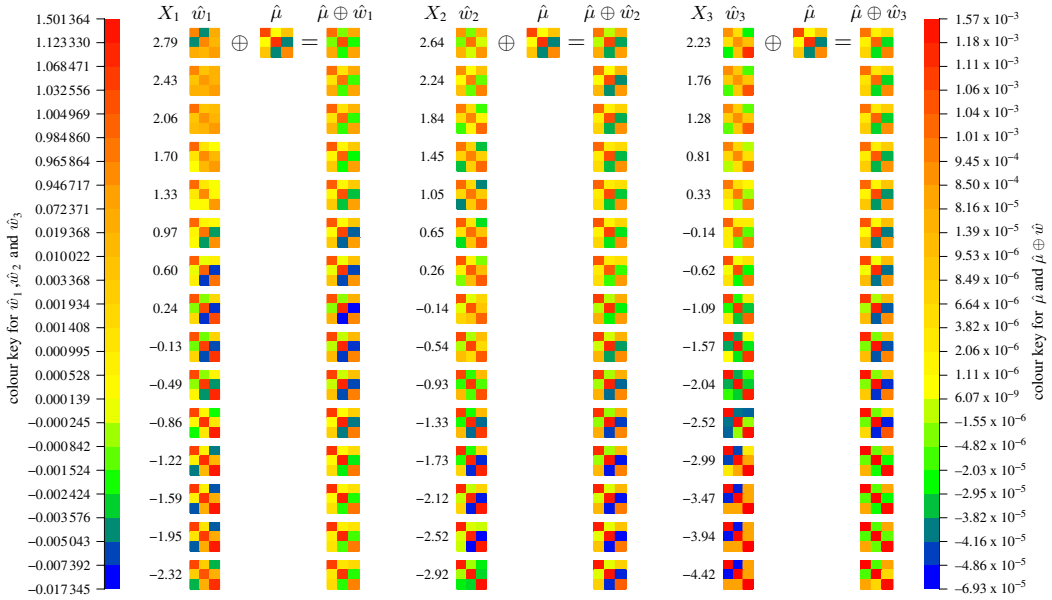

Fig. 2. Estimated additive component functions $\hat{w}_1, \hat{w}_2, \hat{w}_3$ and their effect on the response when other component functions are fixed at identity.

$\mathbb{R}^3$ that was adopted to record the diffusion tensors by $\{e_1, e_2, e_3\}$, so that the matrices presented in Figs. 1 and 2 indicate the coefficients of the corresponding diffusion tensors in this coordinate system. We find that the component functions have distinct effects on the outcome.

Considering, for example, how $\hat{w}_3$, which encodes the fit for language ability as predictor and acts on the average diffusion tensor $\hat{\mu}$ by the group operation $\oplus$, affects the diffusion along the directions e_1 and e_2, we find that they become increasingly negatively correlated as the standardized language ability drops, indicating nonlinear changes in the diffusion that are associated with changing language ability. As a second example, consider $\hat{w}_1$, which encodes the effect of memory. A negative correlation between e_1 and e_2 at high memory levels changes into a positive correlation as memory levels drop in a nonlinear fashion, suggesting distinctive relationships between diffusion patterns and performance scores.

Downloaded from https://academic.oup.com/biomet/article/110/2/361/6730723 by University of California, Davis - Library user on 04 July 2023

This leads to the question of whether the covariates X_k for $k = 1, 2, 3$ are significantly related to the spatially averaged hippocampal diffusion tensor and motivates testing the global null hypothesis

$$H_0 : w_k(x_k) = I_3 \quad \text{for all } x_k, \tag{10}$$

where I_3 denotes the 3×3 identity matrix that is also the group identity of the Lie group $(\mathcal{S}_m^+, \oplus)$ in the log-Euclidean framework, that is, $P \oplus I_3 = P$ for all $P \in \mathcal{S}_3^+$. Corollary 2 can be employed for testing this hypothesis: for a set $\mathbb{H}_k$ of values of X_1, a test based on the asymptotic normality of Corollary 2 can be implemented to obtain the p-value for testing the local null hypothesis $H_0 : w_k(x_k) = I_3$ for each $x_k \in \mathbb{H}_k$, followed by adjustment for multiple comparisons, for example, by the Benjamini–Hochberg method. Here, a natural choice of $\mathbb{H}_k$ is the set of the observed values for X_k in the data. The global null hypothesis (10) is then rejected if at least one adjusted p-value is less than the nominal level α. Implementing this approach and applying it to the ADNI data leads to rejecting the null hypothesis (10) at the level $\alpha = 0.05$ for all $k = 1, 2, 3$, with the minimal corrected p-values 1.028×10^{-9}, 1.80×10^{-5} and $< 10^{-10}$, respectively. This suggests that there are indeed associations between the spatially averaged hippocampal diffusion tensor and memory, executive functioning and language ability.

8. DISCUSSION

There are at least three potential extensions of the proposed methods and theory. First, in the data application we consider the spatially averaged hippocampal diffusion tensor. Although significantly reducing the data noise level, the average may conceal some spatial structure of interest within the hippocampus. One way to address this problem is to view all hippocampal diffusion tensors derived from an image as an $\mathcal{S}_3^+$-valued function $Y : s \mapsto Y(s) \in \mathcal{S}_3^+$ with s ranging over all hippocampal voxels. This functional perspective enables one to borrow information from neighbouring voxels to counter the high-level data noise. However, it is rather challenging to develop an additive model for $\mathcal{S}_3^+$-valued functions (see Dubey & Müller, 2020).

Second, we focus only on the first visit of each subject, and thus do not utilize all available data. To analyse the data of repeated visits that by default are correlated, the theory needs to be extended to account for such correlation, which seems nontrivial, especially when the number of visits may grow with the sample size. Third, when testing hypothesis (10), we perform multiple local tests by using the pointwise asymptotic normality of Corollary 2 and then make corrections for multiple comparisons. This approach, although sufficient for our data application, will be too conservative in general. An alternative method is to develop an asymptotic normality result for the random process $\{\hat{w}_k(x) : x \in \mathcal{X}_k\}$, which may lead to more powerful one-step tests. These extensions are left for future studies.

ACKNOWLEDGEMENT

Lin's research was partially supported by the National University of Singapore (A-0004816-00-00). Müller was supported by the National Science Foundation. Park was supported by the National Research Foundation funded by the Korean government (NRF-2019R1A2C3007355). Data used in the preparation of this article were obtained from the Alzheimer's Disease Neuroimaging Initiative, ADNI, database (adni.loni.usc.edu). As such, the investigators within the ADNI contributed to the design and implementation of ADNI and/or provided

Downloaded from https://academic.oup.com/biomet/article/110/2/361/6730723 by University of California, Davis - Library user on 04 July 2023

data, but did not participate in the analysis or writing of this report. A complete listing of ADNI investigators and funding for ADNI can be found at http://adni.loni.usc.edu/wp-content/uploads/how_to_apply/ADNI_Acknowledgement_List.

Supplementary material

The Supplementary Material contains additional computational details, auxiliary simulation results and proofs. An R implementation of the proposed method is available at: https://www.github.com/linulysses/mam.

References

Afsari, B. (2011). Riemannian L^p center of mass: existence, uniqueness, and convexity. *Proc. Am. Math. Soc.* **139**, 655–73.

Arnaudon, M., Barbaresco, F. & Yang, L. (2013). Riemannian medians and means with applications to radar signal processing. *IEEE J. Sel. Top. Sig. Proces.* **7**, 595–604.

Arsigny, V., Fillard, P., Pennec, X. & Ayache, N. (2006). Log-Euclidean metrics for fast and simple calculus on diffusion tensors. *Magn. Resonance Med.* **56**, 411–21.

Arsigny, V., Fillard, P., Pennec, X. & Ayache, N. (2007). Geometric means in a novel vector space structure on symmetric positive-definite matrices. *SIAM J. Matrix Anal. Applic.* **29**, 328–347.

Barmpoutis, A., Vemuri, B. C., Shepherd, T. M. & Forder, J. R. (2007). Tensor splines for interpolation and approximation of DT-MRI with applications to segmentation of isolated rat hippocampi. *IEEE Trans. Med. Imag.* **26**, 1537–46.

Bhattacharya, R. & Patrangenaru, V. (2003). Large sample theory of intrinsic and extrinsic sample means on manifolds. I. *Ann. Statist.* **31**, 1–29.

Bridson, M. R. & Häfliger, A. (1999). *Metric Spaces of Non-Positive Curvature*. Berlin: Springer.

Bröcker, T. & tom Dieck, T. (1985). *Representations of Compact Lie Groups*. New York: Springer.

Caseiro, R., Henriques, J. F., Martins, P. & Batista, J. (2012). A nonparametric Riemannian framework on tensor field with application to foreground segmentation. *Pat. Recog.* **45**, 3997–4017.

Chau, J. & von Sachs, R. (2019). Intrinsic wavelet regression for surfaces of Hermitian positive definite matrices. *Journal of the American Statistical Association*, Volume 116, Pages 819–832.

Chen, Y. & Müller, H.-G. (2022). Uniform convergence of local Fréchet regression, with applications to locating extrema and time warping for metric-space valued trajectories. *Ann. Statist.* **50**, 1573–92.

Cornea, E., Zhu, H., Kim, P. & Ibrahim, J. G. (2017). Regression models on Riemannian symmetric spaces. *J. R. Statist. Soc.* B **79**, 463–82.

Dai, X. & Müller, H.-G. (2018). Principal component analysis for functional data on Riemannian manifolds and spheres. *Ann. Statist.* **46**, 3334–61.

Davis, B. C., Fletcher, P. T., Bullitt, E. & Joshi, S. (2010). Population shape regression from random design data. *Int. J. Comp. Vis.* **90**, 255–66.

Dryden, I. L., Koloydenko, A. & Zhou, D. (2009). Non-Euclidean statistics for covariance matrices, with applications to diffusion tensor imaging. *Ann. Appl. Statist.* **3**, 1102–23.

Dubey, P. & Müller, H.-G. (2020). Functional models for time-varying random objects. *J. R. Statist. Soc.* B **82**, 275–327.

Eltzner, B., Huckemann, S. & Mardia, K. V. (2018). Torus principal component analysis with applications to RNA structure. *Ann. Appl. Statist.* **12**, 1332–59.

Fillard, P., Arsigny, V., Ayache, N. & Pennec, X. (2005). A Riemannian framework for the processing of tensor-valued images. In *Deep Structure, Singularities, and Computer Vision*, O. Fogh Olsen, L. Florack & A. Kuijper, eds. Berlin: Springer, pp. 112–23.

Fillard, P., Arsigny, V., Pennec, X., Hayashi, K. M., Thompson, P. M. & Ayache, N. (2007). Measuring brain variability by extrapolating sparse tensor fields measured on sulcal lines. *NeuroImage* **34**, 639–50.

Fletcher, P. T. (2013). Geodesic regression and the theory of least squares on Riemannian manifolds. *Int. J. Comp. Vis.* **105**, 171–85.

Fletcher, P. T. & Joshib, S. (2007). Riemannian geometry for the statistical analysis of diffusion tensor data. *Sig. Proces.* **87**, 250–62.

Friston, K. J. (2011). Functional and effective connectivity: a review. *Brain Connect.* **1**, 13–36.

Downloaded from https://academic.oup.com/biomet/article/110/2/361/6730723 by University of California, Davis - Library user on 04 July 2023

GIBBONS, L. E., CARLE, A. C., MACKIN, R. S., HARVEY, D., MUKHERJEE, S., INSEL, P., CURTIS, S. M., MUNGAS, D. & CRANE, P. K. (2012). A composite score for executive functioning, validated in Alzheimer's Disease Neuroimaging Initiative (ADNI) participants with baseline mild cognitive impairment. *Brain Imag. Behav.* **6**, 517–27.

HAN, K., MÜLLER, H.-G. & PARK, B. U. (2020). Additive functional regression for densities as responses. *J. Am. Statist. Assoc.* **115**, 997–1010.

HAN, K. & PARK, B. U. (2018). Smooth backfitting for errors-in-variables additive models. *Ann. Statist.* **46**, 2216–50.

HEIN, M. (2009). Robust nonparametric regression with metric-space valued output. In *Proc. 22nd Int. Conf. Neural Info. Proces. Syst.*, pp. 718–26. Red Hook, NY: Curran Associates.

HINKLE, J., FLETCHER, P. T. & JOSHI, S. (2014). Intrinsic polynomials for regression on Riemannian manifolds. *J. Math. Imag. Vis.* **50**, 32–52.

HUA, X., CHENG, Y., WANG, H., QIN, Y., LI, Y. & ZHANG, W. (2017). Matrix CFAR detectors based on symmetrized Kullback-Leibler and total Kullback-Leibler divergences. *Digit. Sig. Proces.* **69**, 106–16.

HUETTEL, S. A., SONG, A. W. & MCCARTHY, G. (2008). *Functional Magnetic Resonance Imaging*, 2nd ed. Sunderland, MA: Sinauer Associates.

JEON, J. M. & PARK, B. U. (2020). Additive regression with Hilbertian responses. *Ann. Statist.* **48**, 2671–97.

JUNG, S., SCHWARTZMAN, A. & GROISSER, D. (2015). Scaling-rotation distance and interpolation of symmetric positive-definite matrices. *SIAM J. Matrix Anal. Applic.* **36**, 1180–201.

KENDALL, W. S. & LE, H. (2011). Limit theorems for empirical Fréchet means of independent and non-identically distributed manifold-valued random variables. *Braz. J. Prob. Statist.* **25**, 323–52.

LANG, S. (1999). *Fundamentals of Differential Geometry*. New York: Springer.

LE BIHAN, D. (1991). Molecular diffusion nuclear magnetic resonance imaging. *Magn. Resonance Quart.* **7**, 1–30.

LEE, J. M. (2018). *Introduction to Riemannian Manifolds*, vol. 176, 2nd ed. Cham: Springer.

LEE, Y. K., MAMMEN, E. & PARK, B. U. (2010). Backfitting and smooth backfitting for additive quantile models. *Ann. Statist.* **38**, 2857–83.

LEE, Y. K., MAMMEN, E. & PARK, B. U. (2012). Flexible generalized varying coefficient regression models. *Ann. Statist.* **40**, 1906–33.

LENGLET, C., ROUSSON, M., DERICHE, R. & FAUGERAS, O. (2006). Statistics on the manifold of multivariate normal distributions: theory and application to diffusion tensor MRI processing. *J. Math. Imag. Vis.* **25**, 423–44.

LIN, Z. (2019). Riemannian geometry of symmetric positive definite matrices via Cholesky decomposition. *SIAM J. Matrix Anal. Applic.* **40**, 1353–70.

LIN, Z. & MÜLLER, H.-G. (2021). Total variation regularized Fréchet regression for metric-space valued data. *Ann. Statist.* **49**, 3510–33.

LINDBERG, O., WALTERFANG, M., LOOI, J. C., MALYKHIN, N., ÖSTBERG, P., ZANDBELT, B., STYNER, M., VELAKOULIS, D., ÖRNDAHL, E., CAVALLIN, L. et al. (2012). Shape analysis of the hippocampus in Alzheimer's disease and subtypes of frontotemporal lobar degeneration. *J. Alzheimers Dis.* **30**, 355–65.

MAMMEN, E., LINTON, O. & NIELSEN, J. (1999). The existence and asymptotic properties of a backfitting projection algorithm under weak conditions. *Ann. Statist.* **27**, 1443–90.

MOAKHER, M. (2005). A differential geometry approach to the geometric mean of symmetric positive-definite matrices. *SIAM J. Matrix Anal. Applic.* **26**, 735–47.

PARK, B. U., CHEN, C.-J., TAO, W. & MÜLLER, H.-G. (2018). Singular additive models for function to function regression. *Statist. Sinica* **28**, 2497–520.

PELLETIER, B. (2006). Non-parametric regression estimation on closed Riemannian manifolds. *J. Nonparam. Statist.* **18**, 57–67.

PENNEC, X. (2006). Intrinsic statistics on Riemannian manifolds: basic tools for geometric measurements,. *J. Math. Imag. Vis.* **25**, 127–54.

PENNEC, X. (2020). Manifold-valued image processing with SPD matrices. In *Riemannian Geometric Statistics in Medical Image Analysis*, Ed. X. Pennec, S. Sommer and T, Fletcher, pp. 75–134. New York: Academic Press.

PENNEC, X., FILLARD, P. & AYACHE, N. (2006). A Riemannian framework for tensor computing. *Int. J. Comp. Vis.* **66**, 41–66.

PETERSEN, A., DEONI, S. & MÜLLER, H.-G. (2019). Fréchet estimation of time-varying covariance matrices from sparse data, with application to the regional co-evolution of myelination in the developing brain. *Ann. Appl. Statist.* **13**, 393–419.

PIGOLI, D., ASTON, J. A., DRYDEN, I. L. & SECCHI, P. (2014). Distances and inference for covariance operators. *Biometrika* **101**, 409–22.

RATHI, Y., TANNENBAUM, A. & MICHAILOVICH, O. (2007). Segmenting images on the tensor manifold. In *IEEE Conf. Comp. Vis. Pat. Recog.*, Minneapolis, MN, 17–22 June, pp. 1–8. Piscataway, NJ: IEEE Press.

SCHEIPL, F., STAICU, A.-M. & GREVEN, S. (2015). Functional additive mixed models. *J. Comp. Graph. Statist.* **24**, 477–501.

SHAO, L., LIN, Z. & YAO, F. (2022). Intrinsic Riemannian functional data analysis for sparse longitudinal observations. *Ann. Statist.* **50**, 1696–721.

Downloaded from https://academic.oup.com/biomet/article/110/2/361/6730723 by University of California, Davis - Library user on 04 July 2023

Shi, X., Styner, M., Lieberman, J., Ibrahim, J. G., Lin, W. & Zhu, H. (2009). Intrinsic regression models for manifold-valued data. In *Medical Image Computing and Computer-Assisted Intervention - MICCAI*, Ed. G. Z. Yang, D. Hawkes, D. Rueckert, A. Noble and C. Taylor, pp. 192–9. Berlin: Springer.

Steinke, F., Hein, M. & Schölkopf, B. (2010). Nonparametric regression between general Riemannian manifolds. *SIAM J. Imag. Sci.* **3**, 527–63.

Stone, C. J. (1985). Additive regression and other nonparametric models. *Ann. Statist.* **13**, 689–705.

Sturm, K.-T. (2003). Probability measures on metric spaces of nonpositive curvature. In *Heat Kernels and Analysis on Manifolds, Graphs, and Metric Spaces* (Contemp. Math. 338), pp. 357–90. Providence, RI: American Mathematical Society.

Yang, Y. (2007). Globally convergent optimization algorithms on Riemannian manifolds: Uniform framework for unconstrained and constrained optimization. *J. Optimiz. Theory Appl.* **132**, 245–65.

Yu, K., Park, B. U. & Mammen, E. (2008). Smooth backfitting in generalized additive models. *Ann. Statist.* **36**, 228–60.

Yuan, Y., Zhu, H., Lin, W. & Marron, J. S. (2012). Local polynomial regression for symmetric positive definite matrices. *J. R. Statist. Soc.* B **74**, 697–719.

Zhou, D., Dryden, I. L., Koloydenko, A. A., Audenaert, K. M. & Bai, L. (2016). Regularisation, interpolation and visualisation of diffusion tensor images using non-Euclidean statistics. *J. Appl. Statist.* **43**, 943–78.

Zhu, H., Chen, Y., Ibrahim, J. G., Li, Y., Hall, C. & Lin, W. (2009). Intrinsic regression models for positive-definite matrices with applications to diffusion tensor imaging. *J. Am. Statist. Assoc.* **104**, 1203–12.

[*Received on* 17 *February* 2021. *Editorial decision on* 22 *September* 2022]

Downloaded from https://academic.oup.com/biomet/article/110/2/361/6730723 by University of California, Davis - Library user on 04 July 2023

Downloaded from https://academic.oup.com/biomet/article/110/2/361/6730723 by University of California, Davis - Library user on 04 July 2023